Conduction anisotropy, Hall effect, and magnetoresistance of $(TMTSF)_2ReO_4$ at high temperatures

Korin-Hamzić, Bojana; Tafra, Emil; Basletić, Mario; Hamzić, Amir; Untereiner, Gabriele; Dressel, Martin

Source / Izvornik: **Physical review B: Condensed matter and materials physics, 2003, 67**

Journal article, Published version
Rad u časopisu, Objavljena verzija rada (izdavačev PDF)

https://doi.org/10.1103/PhysRevB.67.014513

Permanent link / Trajna poveznica: https://urn.nsk.hr/urn:nbn:hr:217:628201

Conduction anisotropy, Hall effect, and magnetoresistance of $(TMTSF)_2ReO_4$ at high temperatures

Bojana Korin-Hamzić*
Institute of Physics, P.O. Box 304, HR-10001 Zagreb, Croatia

Emil Tafra, Mario Basletić, and Amir Hamzić
Department of Physics, Faculty of Science, P.O. Box 331, HR-10002 Zagreb, Croatia

Gabriele Untereiner and Martin Dressel
1. Physikalisches Institut, Universität Stuttgart, Pfaffenwaldring 57, D-70550 Stuttgart, Germany
(Received 19 July 2002; published 16 January 2003)

We investigated the transport properties of the quasi-one-dimensional organic metal $(TMTSF)_2ReO_4$ above the anion-ordering metal-insulator transition ($T_{AO} \approx 180$ K). The pronounced conductivity anisotropy, a small and smoothly temperature-dependent Hall effect; and a small, positive, and temperature-dependent magnetoresistance are analyzed within the existing Fermi-liquid and non-Fermi-liquid models. We propose that the transport properties of quasi-one-dimensional Bechgaard salts at high temperatures can be described within the Fermi-liquid description.

DOI: 10.1103/PhysRevB.67.014513 PACS number(s): 74.70.Kn, 72.15.Gd, 71.10.Pm

I. INTRODUCTION

Highly anisotropic organic conductors $(TMTSF)_2X$ ($X = PF_6, ClO_4, \ldots$), the so-called Bechgaard salts, exhibit a high conductivity at room temperature and a metallic behavior down to the low temperatures where, under applied pressure and/or magnetic field, their electronic ground states may exhibit a variety of collective effects such as superconductivity, spin-density wave, field induced spin-density wave state with a complex subphase structure, quantum Hall effect, etc.[1] Many of these phenomena are related to the low-dimensional nature of the electronic spectrum. The quasi-one-dimensionality (1D) is a consequence of the crystal structure, in which the TMTSF molecules are stacked in columns (**a** direction) along which the highest conductivity occurs. These parallel columns form sheets that couple in the intermediate conductivity (**b** direction) and form conducting planes. Perpendicular to these planes (along the **c** direction), the coupling is the weakest and consequently this is the least conductivity direction. It is usually taken that the ratios of the resulting conductivity anisotropy and the bandwidth are $\sigma_a:\sigma_b:\sigma_c=(t_a)^2:(t_b)^2:(t_c)^2=10^5:10^3:1$.

There is a long-standing controversy on whether the transport properties of the quasi-1D systems (such as Bechgaard salts) should be understood in terms of the usual Fermi-liquid (FL) theory or the Luttinger-liquid (LL) theory.[2–4] The nature of the metallic phase of interacting electron systems depends strongly on the dimensionality. It is theoretically well established that the conventional FL theory of 3D metals cannot be applied to the interacting electrons whose motion is confined to one dimension. Instead, they form a LL state, with physical properties different from that of a FL, and in which the spin and the charge of an injected electron can move independently. In other words, the quasiparticle excitations that are present in a FL are replaced by separate collective spin and charge excitations, each propagating with a different velocity. LL systems exhibit non-FL-like temperature and energy power-law behavior, and with exponents that are interaction dependent. It is expected that strongly anisotropic Bechgaard salts, with open Fermi surfaces, may exhibit non-FL-like properties at high temperatures (where the thermal energy exceeds the transverse coupling) that lead to the loss of coherence for the interchain transport. The crossover from LL behavior to the coherent one is expected as the temperature (or frequency) is decreased.[5,6]

While many of the low-temperature properties of the Bechgaard salts are well described by the FL theory,[1] their high-temperature phase is still poorly understood. The optical conductivity data were interpreted as a strong evidence for non-FL behavior, and the power-law asymptotic dependence of the high-frequency optical mode has been associated to the LL exponents.[7,8] On the other hand, the interpretation of the transport and magnetic susceptibility results has not been unique, as some data were interpreted in the framework of the LL model,[9,10] whereas for the others, the FL theory was used.[11,12]

Recently, the long missing basic experiment—the temperature dependence of the Hall coefficient in the metallic phase of the quasi-one-dimensional organic conductor $(TMTSF)_2PF_6$—was performed by two groups.[13,14] Their results were obtained for different geometries and were interpreted differently, i.e., using the conventional FL theory[13] and LL concept.[14] More recently, the theoretical calculations of the in-chain and interchain conductivity as well as of the Hall effect in a system of weakly coupled LL chains have been performed,[15,16] giving the explicit expressions as a function of temperature and frequency, but the measurements of dc transport in $(TMTSF)_2PF_6$ along the **c*** axis are not fully understood theoretically from a LL picture.[9,15]

The aim of this paper is to contribute to these, still open, questions about the nature of the metallic state in Bechgaard salts by studying the anisotropic transport properties of yet

another member of the Bechgaard salts family $(TMTSF)_2ReO_4$.

The choice of a salt with $X=ReO_4$ is based on the unified phase diagram, where the anisotropy of the system is varied by changing the anion.[17] In this sense $(TMTSF)_2ReO_4$ is more anisotropic than $(TMTSF)_2PF_6$: the empirical correlations of various structural parameters for a series of $(TMTSF)_2X$ salts were explored[18] by using a van der Waals-like estimate for the radius of the counterion X. The obtained values for the anion radius (at 300 K) clearly show that the maximal value is for the ReO_4^- anion: $R_i(ClO_4^-)=2.64$ Å $<R_i(PF_6^-)=2.81$ Å$<R_i(ReO_4^-)=2.94$ Å. Furthermore, the band structure of $(TMTSF)_2X$ was calculated by the tight-binding scheme,[19] and the values for the ratio of the transfer integrals t_a/t_b at 300 K were 14, 17, and 18 (for $X=PF_6$, ClO_4, and ReO_4, respectively). Therefore, the highest value for $X=ReO_4$ indicates that this salt is more anisotropic than $X=PF_6$.

$(TMTSF)_2ReO_4$ exhibits a metal-insulator anion-ordering transition at $T_{AO}\approx 180$ K.[20] This transition coincides with the periodic ordering of the noncentrosymmetric ReO_4 anions. It is accompanied by a large distortion of the molecular stacks, which doubles the unit cell in all three directions, and consequently gives rise to a sharp increase of the electrical resistivity. We present the high-temperature (above T_{AO}) conductivity results at ambient pressure (for all three current directions), Hall effect in a standard geometry (current parallel to the highest conductivity direction), and magnetoresistance (MR) (in the least conductivity direction). The pronounced conductivity anisotropy, a small and smoothly temperature-dependent Hall effect, and a small, positive, and temperature-dependent MR will be analyzed within the Fermi-liquid and non-Fermi-liquid models. Although not fully conclusive, our data favor the FL description.

II. EXPERIMENT

The measurements were done in the high-temperature region (150 K$<T<$300 K) and in magnetic fields up to 9 T. During the field sweeps, the temperature was stabilized with a capacitance thermometer. All the single crystals used come from the same batch. Their **a** direction is the highest conductivity direction, the **b′** direction (with intermediate conductivity) is perpendicular to **a** in the **a**–**b** plane, and the **c*** direction (with the lowest conductivity) is perpendicular to the **a**–**b** (and **a**–**b′**) plane. The resistivity data, presented here, are for **a**, **b′**, and **c*** axes. For the $\rho_{b'}$ and ρ_{c*} measurements, the samples were cut from a long crystal and the contacts were placed on the opposite **a**–**c*** ($\rho_{b'}$) and **a**–**b′** (ρ_{c*}) surfaces (30-μm-diameter gold wires stuck with silver paint). The samples were cooled slowly (3 K/h) in order to avoid irreversible resistance jumps (caused by microcracks), well known to appear in all organic conductors.

The Hall effect was measured in a standard geometry ($\mathbf{j}\|\mathbf{a},\mathbf{B}\|\mathbf{c}^\star$). Two pairs of Hall contacts and one pair of current contacts were made on the sides of the crystal by evaporating gold pads to which the gold wires were attached with silver paint. An ac current (10 μA to 1 mA, 22 Hz) was used. For $T<T_{AO}$ a dc technique was used because of the large resistance increment. Particular care was taken to ensure the temperature stabilization. The Hall voltage was measured at fixed temperatures and in field sweeps from $-B_{max}$ to $+B_{max}$ in order to eliminate the possible mixing of the magnetoresistance component. At each temperature the Hall voltage was measured for both pairs of Hall contacts to test and/or control the homogeneous current distribution through the sample. The Hall voltage V_{xy} was determined as $[V_{xy}(B)-V_{xy}(-B)]/2$ and the Hall coefficient R_H was obtained as $R_H=(V_{xy}/IB)t$ (I is the current through the crystal and t is the sample thickness). The Hall signal was linear with magnetic field up to 9 T in the whole temperature region investigated.

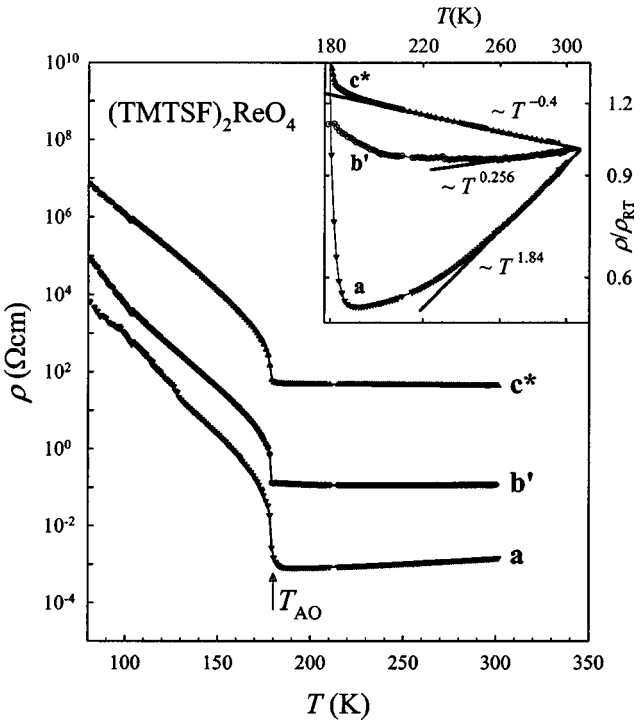

FIG. 1. The temperature dependence of the resistivities $\rho_{\mathbf{a}}$, $\rho_{\mathbf{b}'}$, $\rho_{\mathbf{c}*}$ (measured along the three crystal directions). Inset: log-log plot of $\rho_{\mathbf{a}}$, $\rho_{\mathbf{b}'}$, $\rho_{\mathbf{c}*}$ (normalized to their respective room-temperature values) vs temperature.

The MR, defined as $\Delta\rho/\rho_0=[\rho(B)-\rho(0)]/\rho(0)$, was measured in the $\mathbf{j}\|\mathbf{c}^\star$, $\mathbf{B}\|\mathbf{b}'$ geometry. Single-crystal samples were cut to the required length along the **a** axis with a razor blade and four electrical contacts were made with silver paint. The dimensions along **a**, **b′**, and **c*** for the two samples were $1.197\times0.558\times0.056$ mm^3 and $1.334\times0.553\times0.056$ mm^3, respectively. An ac technique with 10 μA and 22 Hz was used.

III. RESULTS

Figure 1 shows the high-temperature (77 K$<T<$300 K) dependence of the resistivity, measured along the three different crystal directions. The room-temperature resistivity values for $\rho_{\mathbf{a}}(\mathbf{j}\|\mathbf{a})$, $\rho_{\mathbf{b}'}(\mathbf{j}\|\mathbf{b}')$, and $\rho_{\mathbf{c}*}(\mathbf{j}\|\mathbf{c}^\star)$ are 1.45×10^{-3} Ω cm, 0.117 Ω cm, and 44 Ω cm, respectively. A sharp rise of the resistivity below 180 K is a direct manifes-

tation of the anion-ordering (metal-insulator) transition at T_{AO} (the value $T_{AO}=178.8$ K, obtained from the derivatives of our data, is in good agreement with the literature[1]).

Let us now discuss separately the resistivity results for each direction, as they show pronounced differences. These are even more evident from the inset of Fig. 1, where the temperature dependence of resistivity data normalized to their room-temperature values (ρ_{RT}) are given.

The **a**-axis resistivity agrees well with the previously published data.[20] Below T_{AO} the resistivity increases exponentially with an activation energy that can be estimated using the phenomenological law for a simple semiconductor [$\rho \sim \exp(\Delta/k_B T)$]. The obtained value $\Delta=(1000\pm100)$ K is the same for all three current directions. Above T_{AO} the **a**-axis resistivity has a metallicklike behavior, and the decrease of the resistivity between the room temperature down to $T \sim 240$ K can be fitted to a $\rho_{\mathbf{a}} \sim T^{1.84}$ power law. A weaker decrease of the resistivity below $T \sim 240$ K could be ascribed, in our opinion, to the precursor effects due to the anion ordering.

The intermediate-conductivity direction also shows a metallicklike behavior; it is however rather weak, and for only $T>257$ K (i.e., above the minima) it follows a $\rho_{\mathbf{b}'} \sim T^{0.25}$ dependence. At lower temperatures, $\rho_{\mathbf{b}'}$ starts increasing. We point out that, to the best of our knowledge, this is the first time that such a behavior of $\rho_{\mathbf{b}'}$ has been found in a member of the Bechgaard salts family. The resistivity for the $\mathbf{b}'$ axis has been rather poorly investigated up to now. Nevertheless, it is known that for $(TMTSF)_2PF_6$ a monotonic, metallicklike decrease with decreasing temperature follows a $\rho_{\mathbf{b}'} \sim T$ dependence.[21,22]

Finally, for the lowest-conductivity **c*** direction, the resistivity increases with the decreasing temperature, and in the region 190 K$<T<$300 K it follows the $\rho_{\mathbf{c}^*} \sim T^{-0.4}$ law. A similar behavior of $\rho_{\mathbf{c}^*}$ was found for $(TMTSF)_2PF_6$ in the same temperature region, although there is also a well characterized maximum at about 80 K and a metallicklike behavior below.[21,23,24] On the other hand, for $(TMTSF)_2ClO_4$, $\rho_{\mathbf{c}^*}$ shows a metallicklike behavior from room temperature down to the superconducting transition at 1.2 K (in the relaxed state).[12,24]

It should be finally noted that all our data, presented in Fig. 1, are measured at ambient pressure.[4,25] As it is known for most organic conductors, much of the temperature dependence of their conductivity at high temperatures arises from the thermal expansion. Consequently, the constant-pressure data usually show different temperature dependencies than the constant-volume data, and we shall come back to this point when comparing our constant-pressure data with theory, which, in general, makes predictions assuming a constant volume.

Figure 2 shows the temperature dependence of the Hall coefficient R_H of $(TMTSF)_2ReO_4$ above and below T_{AO}. The Hall coefficient is positive in the metallic state, it changes its sign at the transition temperature and increases rapidly with further decrease of the temperature. The inset of Fig. 2 shows in greater details the Hall-effect results in the metallic region, normalized to the calculated R_{H0} value (and this will be discussed more in the following section).

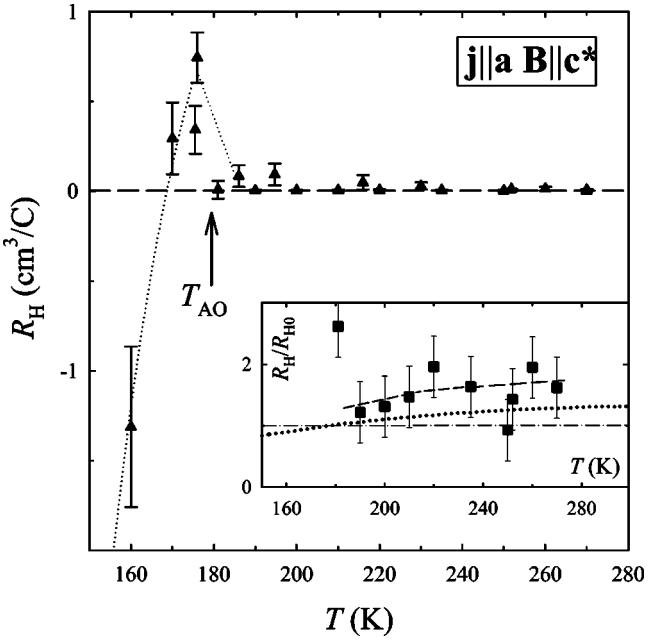

FIG. 2. The temperature dependence of the Hall coefficient R_H. Inset: the normalized Hall coefficient [with R_{H0} given by the Eq. (4)] vs temperature. Dashed line: a guide for the eye; dotted line: $R_H(T)$ behavior predicted in a model where the electron relaxation time varies over the Fermi surface—see text.

The temperature dependence of the transverse MR for $T>180$ K in the least-conducting direction $\mathbf{j}\|\mathbf{c}^\star$, $\mathbf{B}\|\mathbf{b}'$ and with $B=9$ T (obtained on two samples) is presented in Fig. 3. The MR is positive, temperature dependent, and very small (increasing from $\sim 0.02\%$ at room temperature to $\sim 0.1\%$ around 190 K). This particular geometry was chosen because, in the high-temperature region, the MR in the usual

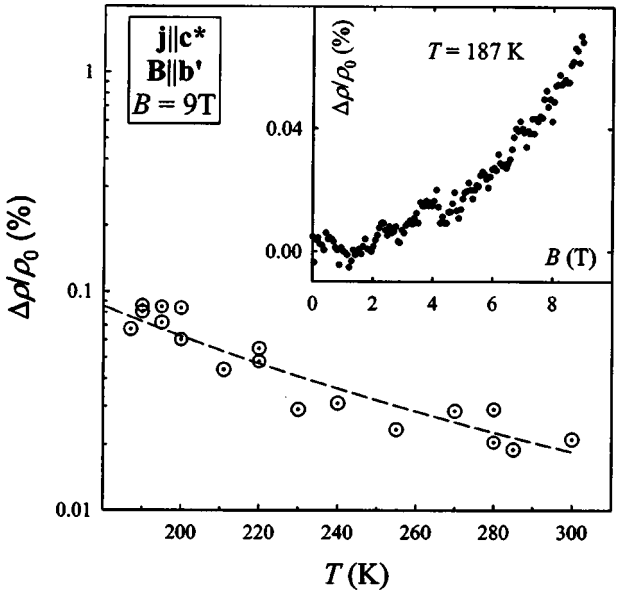

FIG. 3. The temperature dependence of the transverse magnetoresistance $\Delta\rho/\rho_0=\Delta\rho_{\mathbf{c}^*}/\rho_{\mathbf{c}^*}$ in the least-conductivity direction ($\mathbf{j}\|\mathbf{c}^\star$,$\mathbf{B}\|\mathbf{b}'$, $B=9$ T). Dashed line indicates T^{-3} dependence. Inset: $\Delta\rho/\rho_0=\Delta\rho_{\mathbf{c}^*}/\rho_{\mathbf{c}^*}$ vs applied magnetic field at $T=187$ K.

geometry ($\mathbf{j}\|\mathbf{a},\mathbf{B}\|\mathbf{c}^{\star}$) was not detectable. The data below T_{AO} are not given in Fig. 3. Due to the strong increase of the resistivity with the decreasing temperature, it was not possible to measure accurately the MR in that region—namely, small temperature variations resulted in resistance variations larger than those caused by the applied magnetic field, thus yielding to the significant scattering of the data.

In the metallic state of $(TMTSF)_2ReO_4$ at high temperatures, the difference $R(T,B=9\ \mathrm{T})-R(T,B=0)$ is very small, and the only possible way to obtain reliable data was to measure MR at well-stabilized fixed temperatures and with zero-field resistivity compensated before each field sweep. Such a field dependence is shown in the inset of Fig. 3 for $T=187$ K: it is typical for all measured temperatures, showing a B^2 variation.

IV. DISCUSSION

Before entering into a more detailed analysis of the transport measurements of $(TMTSF)_2ReO_4$ in the metallic state (within the existing FL and non-FL models), we should emphasize that the direct comparison of the experimental results with the theoretical predictions is not straightforward. The theoretical calculations are usually done for the constant-volume temperature dependencies, whereas Bechgaard salts in the metallic regime show a large pressure coefficient of the conductivity.[25] In other words, to be able to directly compare the constant-volume $\rho^{(V)}(T)$ theoretical data with the experimental constant-pressure $\rho(T)$ data (shown in Fig. 1), a conversion has to be performed. In our case we have used the same approach as was done for $(TMTSF)_2AsF_6$ (Ref. 4) and $(TMTSF)_2PF_6$,[26] because (to our knowledge) there are no experimental data for the thermal expansion and compressibility of $(TMTSF)_2ReO_4$. However, as ReO_4 is a noncentrosymmetric anion, whereas PF_6 is a centrosymmetric one, such a conversion should be taken with some precaution due to the degree of arbitrariness that underlines the conversion procedure.[27] In the case of $(TMTSF)_2PF_6$, the unit cell at 50 K and at ambient pressure was taken as a reference unit cell—when the temperature T is increased, a pressure P must be applied (at given T) in order to restore the reference volume. Taking into account that in the metallic phase, $\rho_{\mathbf{a}}$ varies 25% per kilobar (for all T values), the measured resistivity $\rho_{\mathbf{a}}$ is then converted into the constant-volume value $\rho_{\mathbf{a}}^{(V)}$ using the expression $\rho_{\mathbf{a}}^{(V)}=\rho_{\mathbf{a}}/(1+0.25P)$.[26] The analogous procedure is applied for $\rho_{\mathbf{b}'}^{(V)}$, because it was found that both σ_a and σ_b increase under pressure at room temperature at a common rate of 25% kbar^{-1} (Refs. 4 and 28) and σ_a/σ_b is essentially T and P independent above $T\approx 25$ K.[4,28] We have therefore converted our data using the same P values as for $(TMTSF)_2PF_6$ and $(TMTSF)_2AsF_6$ that have been calculated from Refs. 4 and 26 and are presented in the inset of Fig. 4. For $\rho_{\mathbf{c}^*}^{(V)}$ the corrections were not made, because the data for $(TMTSF)_2PF_6$ in Ref. 9 were calculated differently. Namely, the variation of $\rho_{\mathbf{c}^*}$ with pressure is not the same for all temperatures, and therefore we could not apply a similar procedure without knowing the exact results for $(TMTSF)_2ReO_4$.

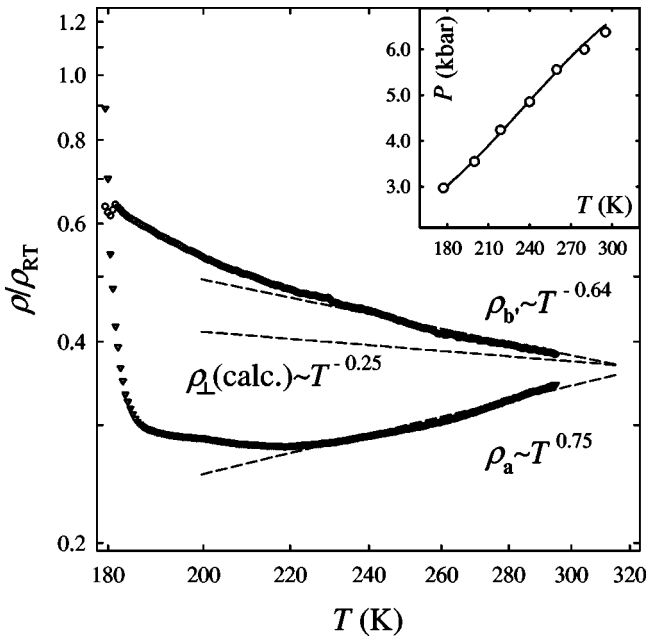

FIG. 4. The temperature dependence of the calculated constant-volume resistivities $\rho_{\mathbf{a}}$ and $\rho_{\mathbf{b}'}$. Also shown is the calculated transverse resistivity $\rho_{\perp}$ in the LL approach (see text for the details). Inset: Temperature dependence of the (effective) pressure P values, deduced from Refs. 4 and 26 and used in our calculation.

The calculated values of constant-volume resistivity for $\rho_{\mathbf{a}}^{(V)}$ and $\rho_{\mathbf{b}'}^{(V)}$ are shown in Fig. 4. The deduced temperature dependencies between ~ 220 K and room temperature are $\rho_{\mathbf{a}}^{(V)}\sim T^{+0.75}$ and $\rho_{\mathbf{b}'}^{(V)}\sim T^{-0.64}$. The comparison of these results with those for $(TMTSF)_2PF_6$ (in the same temperature range,[9,14,22]) shows that a similar behavior is found for $\rho_{\mathbf{a}}^{(V)}$, whereas the $\rho_{\mathbf{b}'}^{(V)}$ data were not calculated and $\rho_{\mathbf{c}^*}^{(V)}\sim T^{-1.4}$. Some important differences between the various Bechgaard salts should be point out. At constant-pressure, $\rho_{\mathbf{b}'}(T)$ for $(TMTSF)_2PF_6$ and $(TMTSF)_2ClO_4$ (Refs. 1 and 29) shows a metalliclike behavior up to room temperature, in contrast to our $\rho_{\mathbf{b}'}(T)$ data for $(TMTSF)_2ReO_4$. On the other hand, while $\rho_{\mathbf{c}^*}(T)$ for $(TMTSF)_2ClO_4$ shows also a metalliclike behavior,[23,24] in the case of $(TMTSF)_2PF_6$, $\rho_{\mathbf{c}^*}(T)$ has a nonmonotonic temperature dependence going through a well-characterized maximum at 80 K. We believe that these differences in $\rho_{\mathbf{b}',\mathbf{c}^*}(T)$ behavior can be ascribed to a higher anisotropy in the $(TMTSF)_2ReO_4$ compound.

The simplest model of electronic transport in metals is the Drude model,[30] where all relaxation processes are described by a single relaxation time τ. The anisotropy of the resistivity values can be accounted for by an anisotropic band mass. Going beyond the Drude model, the scattering rate may be frequency dependent. The simple approach of a homogeneous relaxation rate, however, can still not describe the different T dependencies observed for **a**, **b**′, and **c*** directions; hence it may provide evidence against the conventional FL picture. On the other hand, in $(TMTSF)_2PF_6$, the temperature dependencies of $\rho_{\mathbf{a}}^{(V)}$ (Ref. 31) and the Hall coefficient, between room temperature and down to the lowest temperatures, were quite satisfactory compared with the FL theoret-

ical model where the electron relaxation time varies over the Fermi surface.[32,33] According to this model, in the high-temperature region (where $T>t_c\approx 10$ K and $T<t_b \approx 300$ K) the system is treated as a 2D FL. It is proposed that a quasi-1D conductor behaves like an insulator ($d\rho_{\mathbf{a}}/dT<0$), when its effective dimensionality equals 1, and like a metal ($d\rho_{\mathbf{a}}/dT>0$), when its effective dimensionality is greater than 1. For $(TMTSF)_2ReO_4$ and in the temperature region $T>T_{AO}$, the temperature dependence $\rho_{\mathbf{a}}^{(V)} \sim T^{+0.75}$ and $d\rho_{\mathbf{a}}/dT>0$. This would then imply that $(TMTSF)_2ReO_4$ may also be interpreted in the framework of the same FL model like $(TMTSF)_2PF_6$ (where $\rho_{\mathbf{a}}^{(V)} \sim T^{+0.5}$).[31] In other words, our finding suggests that $(TMTSF)_2ReO_4$ is, like other Bechgaard salts, a 2D anisotropic metal at high temperatures. It should be also pointed out here that the rate of the umklapp scattering along the chains was used for the calculation of $\rho_{\mathbf{a}}^{(V)}$.[33] This relaxation time seems inappropriate for the transport across the chains, but the exact calculations for $\rho_{\mathbf{b}'}^{(V)}$ and $\rho_{\mathbf{c}*}^{(V)}$ have not been performed yet. This is even more important because the temperature dependencies of $\rho_{\mathbf{b}'}^{(V)}$ and $\rho_{\mathbf{c}*}^{(V)}$ for other Bechgaard salts are different. Therefore, the lack of a comprehensive transport theory (with anisotropic relaxation times) prevents us to go further in the comparison of $\rho_{\mathbf{a}}$, $\rho_{\mathbf{b}'}$, and $\rho_{\mathbf{c}*}$ data with the theoretical FL model.

The in-plane conductivity $\sigma_\parallel$, interplane conductivity[15,16] $\sigma_\perp$, and the Hall effect were calculated in a system of weakly coupled Luttinger chains. It was found that the interchain hopping ($t_\perp$ is a perpendicular hopping integral) is responsible for the metallic character of the $(TMTSF)_2X$ compounds, which would be otherwise Mott insulators. The temperature (or the frequency ω) power law was determined, giving for the longitudinal and transverse resistivity, respectively,

$$\rho_\parallel \sim (g_{1/4})^2 T^{16K_\rho - 3}, \tag{1}$$

$$\rho_\perp \sim T^{1-2\alpha}, \tag{2}$$

where $g_{1/4}$ is the coupling constant for the umklapp process with 1/4 filling, K_ρ is the LL exponent controlling the decay of all correlation functions ($K_\rho=1$ corresponds to noninteracting electrons and $K_\rho<0.25$ is the condition upon which the 1/4 filled umklapp process becomes relevant), and $\alpha = 1/4(K_\rho + 1/K_\rho) - 1/2$ is the Fermi-surface exponent.

The comparison of our experimental data, where $\rho_\parallel = \rho_{\mathbf{a}} \sim T^{0.75}$, with the above LL theoretical model yields $K_\rho = 0.234$, the value that is in reasonable agreement with the value $K_\rho = 0.23$ for $(TMTSF)_2PF_6$ obtained from the temperature dependence of $\rho_{\mathbf{a}}(T) \sim T^{0.5}$ in the 100 K$<T<$300 K range.[14,16] For the frequency-dependent conductivity parallel and perpendicular to the chains,

$$\sigma_\parallel \sim \omega^{16K_\rho - 5} \quad \text{and} \quad \sigma_\perp \sim \omega^{2\alpha - 1} \tag{3}$$

is predicted.[15] Optical experiments on $(TMTSF)_2X$ ($X = PF_6$, AsF_6, and ClO_4) along the chains[7,8] yield $K_\rho = 0.23$; the corresponding experiments perpendicular to the chains are in progress.[34] On the other hand, by using $K_\rho = 0.234$, we obtain for the transverse resistivity $\rho_\perp \sim T^{-0.25}$ (shown as dashed line in Fig. 4), while our experimental result gives $\rho_{\mathbf{b}'} \sim T^{-0.64}$. Although it was mentioned previously that the calculated constant-volume results have to be taken with some precautions, the ~ 2.5 times higher exponent value obtained experimentally is nevertheless inconsistent with the predicted one. Here we have to point out that for $(TMTSF)_2PF_6$ it was also concluded that the measurements of the dc transport along the transverse axis are not fully understood theoretically from the LL picture.[35] However, the theoretical model was compared with the **c***-axis resistivity results,[9,15] which, in our opinion, is not the best choice: the comparison should be applied to t_b and $\rho_{\mathbf{b}'}$ in the first place, rather than to t_c and $\rho_{\mathbf{c}*}$, because $t_b \gg t_c$.

The conclusion of this part of the work therefore is that the resistivity results for $(TMTSF)_2ReO_4$ can be well explained within the framework of both FL and LL models, but only for the **a**-axis. This is because there is no comprehensive theoretical FL transport approach (with anisotropic relaxation times) for $\rho_{\mathbf{b}'}(T)$ and $\rho_{\mathbf{c}*}(T)$, and on the other hand, the power law for the temperature-dependent transverse resistivity, proposed in the LL model, does not agree with our $\rho_{\mathbf{b}'}(T)$ experimental results.

In the metallic state, the Hall coefficient R_H (Fig. 2) is small, positive (holelike), and slightly temperature dependent. In the vicinity of the T_{AO} phase transition, some enhancement in the $R_H(T)$ behavior can be observed (due to a pronounced scattering of the measured values, the error bars are large in this region). The Hall coefficient changes its sign below T_{AO} and becomes negative (electronlike). For $T<T_{AO}$, $|R_H(T)|$ also shows a rapid increase with decreasing temperature, i.e., the Hall resistance is activated, as expected for a semiconductor with the activation energy corresponding to that of the resistivity. In the inset of Fig. 2 the same results of the metallic region are shown in greater detail but normalized to the expected Hall-coefficient constant value $R_{H0} = 3.5\times 10^{-3}\text{cm}^3/\text{A s}$. The dashed line in the inset is a guide to the eye. The R_{H0} value is obtained using the tight-binding dispersion along the chains (the band is 1/4 filled by holes and the scattering time τ is constant over the Fermi surface) yielding[36,37]

$$R_{H0} = \frac{1}{ne}\frac{k_F a}{\tan(k_F a)}, \tag{4}$$

where e and n are the electric charge and concentration of the carriers and $k_F a = \pi/4$. The carrier density of 1 hole/f.u. gives $n = 1.4\times 10^{21}\text{cm}^{-3}$. As seen from the figure, the experimental results for R_H are, around 200 K, quite close to the expected R_{H0} value, and show an increase of $\sim 30\%$ at room temperature.

It has been shown[16] that the Hall coefficient R_H of a system of weakly coupled LL chains, with the magnetic field perpendicular to the chains and in the absence of the in-chain momentum relaxation, is independent of frequency or temperature. Moreover, R_H is given by a simple expression, corresponding to the noninteracting fermions, i.e., $R_H = R_{H0}$. The temperature dependence of R_H could be addressed theoretically once the in-chain momentum relaxation processes

are included,[16] but the detailed calculations along these lines have not been done up to now. From this point of view, our $R_H(T)$ results for $T>200$ K, with a weak temperature dependence and with the values scattered about $\pm 20\%$ around the R_{H0} value, cannot exclude the possible LL interpretation.

However, the controversy with the LL theoretical model arises from the number of carriers participating in the dc transport. Namely, from the optical conductivity results for $(TMTSF)_2X$ salts[7,8] (considered as the strong evidence for the LL behavior), it was concluded that all the dc transport is due to a very narrow Drude peak containing only 1% of the spectral weight (arising from interchain hopping), whereas the remaining of 99% is above an energy gap (of the order of 200 cm^{-1}), reminiscent of a Mott insulating structure. Such a reduction of the carrier concentration n participating in the dc transport should give a factor of 100 higher R_H value, for both calculated R_{H0} and experimentally obtained values. It should be noted that this point was also established[13] for the Hall effect in $(TMTSF)_2PF_6$. However, these measurements were done in a different geometry (with respect to our data), and the temperature-independent Hall coefficient leads to the explanation in the framework of the FL theory with isotropic τ.

It has also been shown[32] that R_H may be temperature dependent in a model where the electronic relaxation time varies over the Fermi surface, i.e., the same model that satisfactorily describes $\rho_{\mathbf{a}}$. The Hall coefficient then consists of two terms: $R_H=R_H^{(0)}+R_H^{(1)}$, where the first term is a temperature-independent band-structure contribution R_{H0}, and the second term is the temperature-dependent contribution determined by the variation of the relaxation time $\tau(k_y)$ over the (Fermi surface) FS.[33] It was found that R_H is strongly temperature dependent at low temperatures, while at high temperatures ($T \geqslant t_b$) it saturates at the R_{H0} value. The experimental results for $R_H(T)$ and $\rho_{\mathbf{a}}(T)$ for $(TMTSF)_2PF_6$ (that were previously explained by the LL concept[14]) were quantitatively compared with this model and a reasonably good agreement was found.[31] In this model, however, the anion-ordering transition has not been taken into account, and we can compare it with our experimental results only for $T>200$ K. The dotted line in the inset of Fig. 4 shows the theoretically predicted $R_H(T)\sim T^{0.7}$ behavior [cf. Fig. 2(a) in Ref. 32] (obtained with the electron tunnelling amplitudes between the nearest and next-nearest chains $t_b=300$ K and $t_{b'}=30$ K, respectively). As seen from Fig. 2, the temperature dependence of $R_H(T)$ as well as the experimental values (albeit somehow higher) satisfactorily follow the predicted Fermi-liquid description with an anisotropic relaxation time τ.

The temperature dependence of the transverse MR for $T>180$ K, and for the particularly chosen geometry $(\mathbf{j}\|\mathbf{c}^\star,\mathbf{B}\|\mathbf{b}')$ presented in Fig. 3, exhibits a $\Delta\rho_{\mathbf{c}*}/\rho_{\mathbf{c}*}\sim T^{-3}$ behavior. Our choice of geometry follows the prediction obtained in the simple FL model that is based on the band theory describing the transport at the open FS in the relaxation-time approximation, i.e., for the isotropic τ.[23,24] Although we are aware that the isotropic τ is a rather crude approximation for highly anisotropic systems such as Bechgaard salts, we will compare our results with this model, as there are no published calculations for an anisotropic τ. When the magnetic field B is along the lowest-conductivity direction **c***, the low-field MR for the highest-conductivity direction (**a**) is given by $\Delta\rho_{\mathbf{a}}/\rho_{\mathbf{a}}\sim(\omega_{\mathbf{a}}\tau)^2$ ($\omega_{\mathbf{a}}$ is the cyclotron frequency associated with the electron motion along the **a** axis, obtained in the model as $\omega_{\mathbf{a}}\approx\omega_{\mathbf{c}*}t_b/t_a$). The largest effect is expected for the current along the **c*** axis and B along the intermediate conductivity $\mathbf{b}'$ axis, because in this case $\Delta\rho_{\mathbf{c}*}/\rho_{\mathbf{c}*}\sim(\omega_{\mathbf{c}*}\tau)^2$ [where $\omega_{\mathbf{c}*}=(1/c_0\hbar)eBcv_a$, c_0 is the velocity of light, $\hbar$ is the Planck constant, c is the lattice parameter, and v_a is the Fermi velocity along the chains]. It is evident that in this case $\omega_{\mathbf{c}*}\gg\omega_{\mathbf{a}}$. Indeed, in the high-temperature region, the MR in the usual geometry $(\mathbf{j}\|\mathbf{a},\mathbf{B}\|\mathbf{c}^\star)$ was not detectable (it was within the present resolution of our setup), while for this particular geometry $(\mathbf{j}\|\mathbf{c}^\star,\mathbf{B}\|\mathbf{b}')$, we obtained reliable results. Using the above simple relation (with the lattice parameter[1] $c=13.48$ Å), the experimentally measured value $\Delta\rho_{\mathbf{c}*}/\rho_{\mathbf{c}*}\approx 0.02\%$ at 300 K gives for the mean free path along the chains $l_{\mathbf{a}}=v_{\mathbf{a}}\tau=7.62$ Å. Knowing that the molecular spacing along the chains is $a=3.64$ Å, it then follows that $l_{\mathbf{a}}\approx 2.1a$, which implies a coherent in-chain carrier propagation (because $l_{\mathbf{a}}>a$). On the other hand, the $\rho_{\mathbf{b}'}(T)$ (below 257 K) and the $\rho_{\mathbf{c}*}(T)$ results suggest diffusive interchain carrier propagation. As already mentioned, with respect to $(TMTSF)_2ClO_4$ and $(TMTSF)_2PF_6$, the $\rho_{\mathbf{b}'}(T)$ and $\rho_{\mathbf{c}*}(T)$ variations in $(TMTSF)_2ReO_4$ are also different. From this point of view, the surprising result emerges from the comparison of our present results for $(TMTSF)_2ReO_4$ with those for $(TMTSF)_2ClO_4$ and $(TMTSF)_2PF_6$, obtained for the same geometry.[12] This is shown in Fig. 5, where the data for all three systems are given as $(\Delta\rho_{\mathbf{c}*}/\rho_{\mathbf{c}*})^{1/2}$ vs temperature.

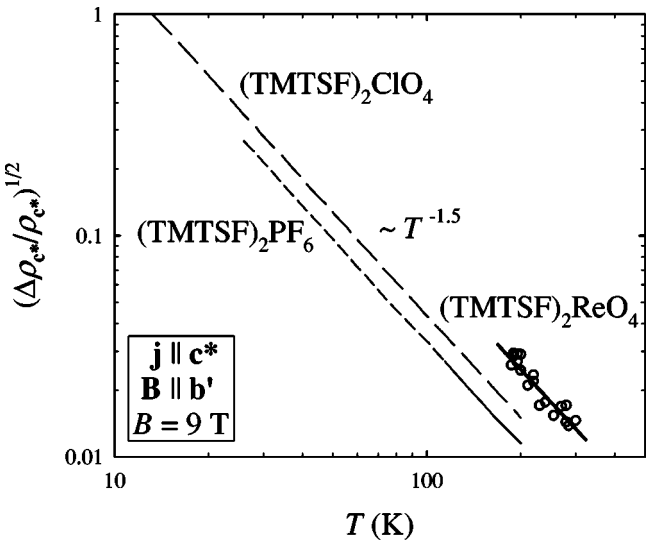

FIG. 5. The temperature dependence of the transverse magnetoresistivity $(\Delta\rho_{\mathbf{c}*}/\rho_{\mathbf{c}*})^{1/2}$. Also shown are the data for $(TMTSF)_2ClO_4$ and $(TMTSF)_2PF_6$ (both from Ref. 12 and normalized to 9 T). The data for $(TMTSF)_2PF_6$ above 110 K are our unpublished results.

The different $\rho_{c*}(T)$ behavior in different salts obviously does not influence the $\Delta\rho_{c*}/\rho_{c*}$ vs T dependence. The similarity between the presented data, i.e., the same temperature dependence, is more than evident, and all three salts follow a $(\Delta\rho_{c*}/\rho_{c*})^{1/2}\sim T^{-1.5}$ variation (or, if using the above simple band picture, $\tau\sim T^{-1.5}$). Moreover, for $(TMTSF)_2ClO_4$ and $(TMTSF)_2PF_6$, the same temperature dependence of the MR is also obtained at low temperatures,[12] i.e., far below the temperature ($\sim$100 K) where the drastic changes in the physical properties are to be expected, due to the 1D$\rightarrow$2D dimensionality crossover from the LL to a coherent FL behavior, as the temperature is lowered.[6,35] In line with these, the possible interpretation of our MR results is that the scattering mechanism, which governs the transport in the least-conducting direction, remains unchanged over the entire temperature range that rules out any temperature induced interlayer decoupling. The diffusive (i.e., the incoherent) interchain transport then assures a coupling between the chains strong enough to allow the FL description for the transport properties at high temperatures in Bechgaard salts. On the other hand, the possible appearance of the LL features in the transport properties should be expected in the more anisotropic $(TMTTF)_2X$ series, where the interactions play a crucial role.[4,35]

In conclusion, we performed the transport measurements in the metallic state of $(TMTSF)_2ReO_4$. The resistivity results for the **a** axis may be well explained in the framework of both FL and LL models. On the other hand, the $\rho_{b'}(T)$ and $\rho_{c*}(T)$ resistivity data do not agree with the prediction from the LL model, whereas the lack of a comprehensive FL transport theory (with anisotropic relaxation times) prevents us from reaching the final conclusion concerning the FL approach. The Hall-effect data suggest that the FL description with anisotropic τ remains valid throughout the metallic state. Finally, the magnetoresistance measurements do not give evidence of different regimes in the normal state of the Bechgaard salts, which can be related to the 1D$\rightarrow$2D dimensionality crossover from the LL to a coherent FL behavior. Our final proposal, therefore, is that the Fermi-liquid model with anisotropic relaxation, i.e., the direction-dependent relaxation, should apply for the transport properties in Bechgaard salts.

ACKNOWLEDGMENT

Part of the work was supported by the Deutsche Forschungsgemeinschaft (DFG) under Grant No. Dr 228/10.

*Electronic address: bhamzic@ifs.hr

[1] T. Ishiguro, K. Yamaji, and G. Saito, *Organic Superconductors*, 2nd ed. (Springer, Berlin, 1998).
[2] H.J. Schulz, Int. J. Mod. Phys. B **5**, 57 (1991).
[3] J. Voit, Phys. Rev. B **47**, 6740 (1992).
[4] D. Jérome, in *Organic Conductors*, edited by J. Farges (Dekker, New York, 1994), p. 405.
[5] C. Bourbonnais, F. Creuzet, D. Jérome, K. Bechgaard, and A. Moradpour, J. Phys. (France) Lett. **45**, L755 (1984).
[6] S. Biermann, A. Georges, A. Lichtenstein, and T. Giamarchi, Phys. Rev. Lett. **87**, 276405 (2001).
[7] M. Dressel, A. Schwartz, G. Grüner, and L. Degiorgi, Phys. Rev. Lett. **77**, 398 (1996).
[8] A. Schwartz, M. Dressel, G. Grüner, V. Vescoli, L. Degiorgi, and T. Giamarchi, Phys. Rev. B **58**, 1261 (1998).
[9] J. Moser, M. Gabay, P. Auban-Senzier, D. Jérome, K. Bechgaard, and J.M. Fabre, Eur. Phys. J. B **1**, 39 (1998).
[10] M. Dumm, A. Loidl, B.W. Fravel, K.P. Starkey, L.K. Montgomery, and M. Dressel, Phys. Rev. B **61**, 511 (2000).
[11] M. Miljak, J.R. Cooper, and K. Bechgaard, Phys. Rev. B **37**, 4970 (1988).
[12] J.R. Cooper, L. Forró, B. Korin-Hamzić, K. Bechgaard, and A. Moradpour, Phys. Rev. B **33**, 6810 (1986).
[13] G. Mihály, I. Kézsmárki, F. Zámborszky, and L. Forró, Phys. Rev. Lett. **84**, 2670 (2000).
[14] J. Moser, J.R. Cooper, D. Jérome, B. Alavi, S.E. Brown, and K. Bechgaard, Phys. Rev. Lett. **84**, 2674 (2000).
[15] A. Georges, T. Giamarchi, and N. Sandler, Phys. Rev. B **61**, 16 393 (2000).
[16] A. Lopatin, A. Georges, and T. Giamarchi, Phys. Rev. B **63**, 075109 (2001).
[17] D. Jérome, Science **252**, 1509 (1991).
[18] T.J. Kistenmacher, Mol. Cryst. Liq. Cryst. **136**, 361 (1986).
[19] P.M. Grant, J. Phys. (Paris), Colloq. **44**, C3-847 (1983).
[20] C.S. Jacobsen, H.J. Pedersen, K. Mortensen, G. Rindorf, N. Thorup, J.B. Torrance, and K. Bechgaard, J. Phys. C: Solid State Phys. **15**, 2657 (1982).
[21] K. Bechgaard, C.S. Jacobsen, K. Mortensen, H.J. Pedersen, and N. Thorup, Solid State Commun. **33**, 1119 (1980).
[22] J. Moser, Ph.D. thesis, University of Paris XI, 1999.
[23] J.R. Cooper, L. Forró, and B. Korin-Hamzić, Mol. Cryst. Liq. Cryst. **119**, 121 (1985).
[24] B. Korin-Hamzić, L. Forró, and J.R. Cooper, Mol. Cryst. Liq. Cryst. **119**, 135 (1985).
[25] D. Jérome and H.J. Schulz, Adv. Phys. **31**, 299 (1982).
[26] P. Auban-Senzier, D. Jérome, and J. Moser, in *Physical Phenomena at High Magnetic Fields III*, edited by Z. Fisk, L. Gor'kov, and R. Schrieffer (World Scientific, Singapore, 1999), p. 211.
[27] C. Burbonnais and D. Jérome, in *Advances in Synthetic Metals, Twenty Years of Progress in Science and Technology*, edited by P. Bernier, S. Lefrant, and G. Bidan (Elsevier, New York, 1999), p. 206.
[28] H.J. Schulz, D. Jérome, A. Mazaud, M. Ribault, and K. Bechgaard, J. Phys. (Paris) **42**, 991 (1981).
[29] J. R. Copper and B. Korin-Hamzić, in *Organic Conductors* (Ref. 4), p. 359.
[30] M. Dressel and G. Grüner, *Electrodynamics of Solids* (Cambridge University Press, Cambridge, 2002).
[31] V.M. Yakovenko and A.T. Zheleznyak, Synth. Met. **120**, 1083 (2001).
[32] V.M. Yakovenko and A.T. Zheleznyak, Synth. Met. **103**, 2202 (1999).
[33] A.T. Zheleznyak and V.M. Yakovenko, Eur. Phys. J. B **11**, 385 (1999).
[34] K. Petukhov and M. Dressel (unpublished).
[35] S. Biermann, A. Georges, T. Giamarchi, and A. Lichtenstein, in

Strongly Correlated Fermions and Bosons in Low-Dimensional Diordered Systems, Vol. 72, of NATO Science Series II, edited by I.V. Lerner, B.L. Althsuler, V.I. Fal'ko, and T. Giamarchi (Kluwer Academic, Dordrecht, The Netherlands, 2002).

[36] J.R. Cooper, M. Miljak, G. Delpanque, D. Jérome, M. Wagner, J.M. Fabre, and L. Giral, J. Phys. (Paris) **38**, 1097 (1977).

[37] K. Maki and A. Virosztek, Phys. Rev. B **41**, 557 (1990).